



## Study of the Effects of Five Different Machining Fluids on the Surface Hardness and Corrosion Behaviour of Al6061 Alloy

Imhade Princess Okokpujie<sup>1,2,\*</sup>, Jude Ebieladoh Sinebe<sup>3</sup>, Lagouge Kwanda Tartibu<sup>1</sup>

<sup>1</sup> Department of Mechanical and Industrial Engineering Technology, University of Johannesburg, Johannesburg, 2028, South Africa

<sup>2</sup> Department of Mechanical and Mechatronics Engineering, Afe Babalola University, Ado Ekiti, 360001, Nigeria

<sup>3</sup> Department of Mechanical Engineering, Delta State University, Delta State, Abraka, 330105, Nigeria

### ARTICLE INFO

#### Article history:

Received 21 July 2023

Received in revised form 4 October 2023

Accepted 15 November 2023

Available online 3 April 2024

#### Keywords:

Al6061 alloy; Corrosion; Machining fluids; Surface hardness

### ABSTRACT

The effects of various machining fluids on the surface hardness and corrosion behaviour of Al6061 alloy were investigated in this study. The study employed the two-step method to develop the machining fluid containing TiO<sub>2</sub> nanoparticles with various percentage concentrations. The corrosion study media consists of soluble oil (sample A1), mineral oil (sample A2), 0.2-g/l-TiO<sub>2</sub> nano-mineral machining fluid (sample A3), 0.4-g/l-TiO<sub>2</sub> nano-mineral machining fluid (sample A4) and 0.6-g/l-TiO<sub>2</sub> nano-mineral machining fluid (sample 5). The corrosion study was carried out using potentiodynamic corrosion and polarisation resistance techniques. After the corrosion study, the SEM and EDS were employed to investigate the microstructure and elemental composition of the machining fluid effects on the Al6061 alloy, and the Vickers micro-hardness machine was used to test the surface hardness of the normal face region that was exposed to the corrosion study. The results show that the soluble oil has a high corrosion rate, with the list polarisation resistance rate compared to the other machining fluid employed in this study. Furthermore, the 0.6-g/l-TiO<sub>2</sub> nano-mineral machining fluid has the lowest corrosion rate of 0.115 (µm/year) and the highest polarisation resistance of 1.543 (MΩ). The study concluded that the 0.6-g/l-TiO<sub>2</sub> nano-mineral machining fluid is viable for the machining process.

## 1. Introduction

A popular material in the family of aluminium alloys for structural applications is aluminium 6061 alloy (Al6061), which has a high strength-to-weight ratio and strong corrosion resistance [1]. Traditionally, Al6061 components have been produced using methods like casting, forging, rolling, and machining, which generate a lot of scrap and waste. Advanced additive manufacturing (AM) methods have made it possible to redesign components to have near-net forms with less material waste [2]. Sayuti *et al.* [3] investigated the optimum SiO<sub>2</sub> nano lubrication parameters in end milling of aerospace Al6061-T6 alloy. A notable benefit would be the CNC milling machine's capacity to produce orders in batches.

\* Corresponding author.

E-mail address: [lp.okokpujie@abuad.edu.ng](mailto:lp.okokpujie@abuad.edu.ng)

<https://doi.org/10.37934/araset.42.2.7288>

However, because it impacts the product's look, functionality, and dependability, the demand for high quality emphasises product quality, particularly the roughness of the machined surface. Correct lubrication might enhance the tribological properties of Al6061-T6, resulting in greater product quality. To achieve the proper lubrication conditions for the lowest cutting force, cutting temperature, and surface roughness, the best SiO<sub>2</sub> nano-lubrication parameters for milling Al6061-T6 are examined in this research.

The machining fluid in computer numerical control (CNC) systems is very significant because it assists in reducing the heat generated during cutting operation at the act of the machining region. However, many machining fluids have been developed and employed in the machining process. Still, most of them are not ecologically friendly, and most studies that developed machining fluid do not check for its effects in terms of corrosion on the workpiece. Therefore, Machining involves eliminating undesirable material from a workpiece by moving a tool against it [4,5]. Cutting fluids are used in metalworking and machining operations to increase tool life, boost material quality, and benefit the machining process [6]. A novel class of cutting fluids known as "nano-cutting fluids" was developed by mixing a base fluid with nanomaterials such as nanoparticles, nanorods, and nanotubes [7,8]. Agricultural wastes can be used to make these nanoparticles because doing so is more economical and environmentally friendly than expensive and harmful materials [9]. According to Okokpujie *et al.*, [10], the art of environmentally friendly manufacturing of mechanical components for use in aerospace and defence technology is nano-lubricant machining of aluminium 8112 alloys. However, because of the workpiece's material adherence to the cutting tool, machining aluminium alloys tend to produce too much heat, raising the cutting force (F.C.). The problem has prompted researchers to consider implementing nano-lubrication techniques. This research compared the effects of eco-friendly TiO<sub>2</sub> and MWCNT nano-lubricants on cutting force when the aluminium 8112 alloys were machined. Before machining, nanoparticles were added to the base oil using a magnetic stirrer and an ultrasonic vibrator as part of the minimum quantity lubrication procedure. The investigation used 50 tests of quadratic central composite designs with five components at five levels. The input parameters include Helix angle, spindle speed, axial depth of cut, feed rate, and cutting length. According to the findings, adding nanoparticles improves how well vegetable oil performs regarding cutting force. Comparing TiO<sub>2</sub> nano-lubricant to MWCNTs and vegetable oil, respectively, shows that the TiO<sub>2</sub> nanoparticles solution causes a reduction in cutting force. However, this study did not validate whether the TiO<sub>2</sub> machining fluid can affect the workpiece life via corrosion of the machining surface. Therefore, the need to study the effects of various volume concentrations of TiO<sub>2</sub> machining fluid on the surface and properties of aluminium alloys is needed. This study stands to proffer a solution to this area of research. The study's findings indicate that the type of cutting procedure impacts the cut surface's hardness and surface quality. The kind of cutting procedure impacts the microstructure of cut surfaces. All cutting processes, excluding abrasive water jet, cause microstructural changes in the cut materials. The abrasive water jet approach can be employed successfully in industrial applications requiring minimal microstructural changes and hardness reduction [11]. Al 6061 is one of the 6000 series aluminium alloys used in valves, couplings, bicycle frames, camera lenses, brake components, aircraft and aerospace components, marine fittings, and other items. Al 6061 comprises 0.63% Si, 0.466% Fe, 0.096% Cu, 0.179% Mn, 0.53% Mg, 0.091% Zn, 0.028% Cr, and 0.028% Ti, with the remaining portion being aluminium. Young's modulus is 80 G pa, with a BHN hardness 98. A rectangular bar measuring 600x50x10mm was employed in this study [12].

According to polarisation research, composites have greater corrosion resistance than matrix alloys. The excellent bond fidelity of TiC particulates with aluminium and potential electrochemical decoupling between TiC particles and Al 6061 matrix alloy is credited with the observed enhancement in the corrosion resistance of TiC particulate reinforced composites. The EIS

investigation shows that the corrosion process is mainly controlled by charge transfer and that the polarisation resistance ( $R_p$ ) increases with increasing TiC concentration in composites. It has been established that titanium carbide is a viable reinforcement for Al MMCs to increase their corrosion resistance [13]. Magnesium and silicon are the main alloying components of aluminium 6061, a precipitation-hardened metal alloy. The yield strength and ultimate tensile strength of T6 temper 6061 are at least 240 MPa (35,000 psi) and 290 MPa (42,000 psi), respectively. The 310 MPa (45 ksi) and 270 MPa (39 ksi), respectively, are normal. It is difficult to control or eliminate corrosion since it occurs continuously. Magnesium and Silicon are the main alloying ingredients in this hardened aluminium alloy. This study analyses how corrosion occurs when aluminium 6061-T6 reacts with acidic, alkaline, and salty environments. It will become apparent by examining the comparative results that the Aluminium 6061 T6 alloy has higher.

Corrosion is a significant area that manufacturers look into when developing engineering products [14]. However, to validate that a machining fluid is viable for the cutting process, the analysis of the effects of the machining fluid on the surface hardness and the study of the corrosion effects on the workpiece is highly needed. The use of nano-machining fluids causes the cutting forces for machining operations, including grinding, milling, turning, and drilling, to be diminished. The properties of the employed nanoparticles impact this reduction [15]. Machining fluids helps save money by preventing and reducing costs associated with tool wear, corrosion, built-up edges, and machining time. Numerous factors related to machining fluids, including pressure, application technique, cutting fluid flow rate, impact tool [16-,17]. Wagri *et al.*, [19], the surface integrity of hardened AISI 4140 steel was studied while being turned using a scalable pulsed power plasma SPPP-ALTiSiN coated carbide tool with minimal quantity lubrication (MQL) assistance from nanofluids. Radiator coolant and zinc oxide nanoparticles are combined to create nano-cutting fluid. In hard turning, RSM was employed to optimise the surface roughness. The outcomes of the predictive modelling are then used for economic analysis. Due to minimal tool wear and increased cutting edge's effective length, the machined surface quality improved when the nose radius was increased. The tool life of the SPPP-ALTiSiN coated carbide insert is reported as 46 minutes under nanofluid-MQL at ideal cutting circumstances. As a result, it projected the entire machining cost per component to be Rs.23.12 in Indian rupees. In the study carried out by Wagri *et al.* [19], it was confirmed that the hardness of a material significantly impacts its machinability, which in turn impacts the component's surface quality, power consumption, and cutting tool life [20]. However, the current machining fluid employed in the industry, e.g., soluble oil, is not environmentally friendly. It has some side effects on the surface roughness of the workpiece during the machining process. Hence there is need for the study to validate the corrosion properties of the developed  $TiO_2$  nano-machining fluid during the cutting of Al6061 alloys

The aim is to study the effects of various nano-machining fluids on the surface hardness and corrosion behaviour of Al6061 alloy. Moreover, to achieve the aim.

The study has the following objectives, which are to:

- i. Develop the different volume concentrations of the  $TiO_2$  nano-machining fluid for the corrosion study.
- ii. Study the effects of nano-machining fluid on the surface hardness and corrosion rate of the Al6061 alloys.
- iii. Carryout comparative analysis of the developed  $TiO_2$  nano-machining fluid with the base fluid and the conventional machining fluid

This study will increase the implementation of the rate of machining fluid in the manufacturing industry. When the validation of the developed different concentrations of the TiO<sub>2</sub> nano-machining lubricant is analysed and compared with the soluble oil, the mineral oil in a corrosion experiment using electrochemical and gravimetric techniques proves viable. It will also reduce the application of excess machining fluid during the cutting process, so the tribological properties in heat exchange have been significantly improved.

## 2. Methodology

### 2.1 Materials

This section entails the materials employed for this study. The Al 6061 alloy and its chemical composition are presented in Table 1 and Figure 1.

**Table 1**

Composition of the aluminium alloy material in %

Materials	Fe	Si	Mn	Cu	Zn	Mg	Pb	Sn	Al
Wt. (%)	1.27	2.448	0.108	0.434	0.492	0.2	0.112	0.073	94.87

The TiO<sub>2</sub> nanoparticles used to develop the machining fluid are presented in Figure 1b. Also, the mineral oil used as the based fluid is given in Figure 1c.

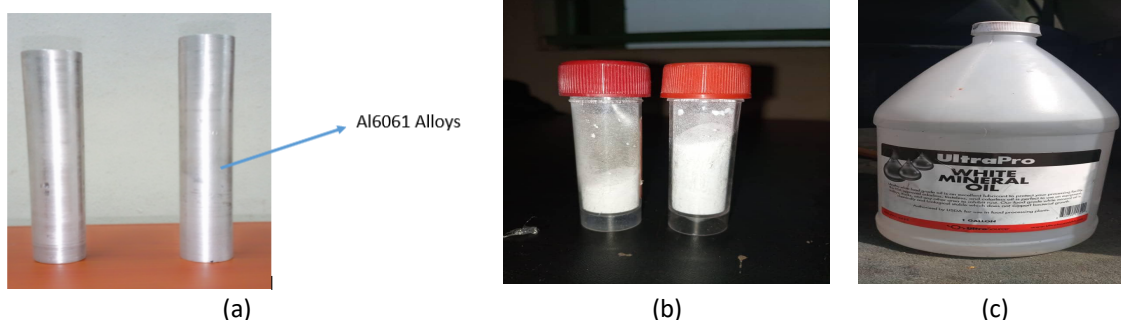


**Fig. 1.** (a) Image of the aluminium workpieces, (b) The TiO<sub>2</sub> nanoparticles, and (c) The white mineral oil

The SEM and EDX analysis showing the microstructural analysis and the chemical composition of the TiO<sub>2</sub> nanoparticles is presented in Figure 2. The SEM and EDS analysis of the TiO<sub>2</sub> nano-powder used in preparing the nano-lubricant is shown in Figure 2(a-b). The EDS analysis confirmed that the chemical composition of the nano-powders is 99.7% titanium-oxide (TiO<sub>2</sub>). The morphology of the TiO<sub>2</sub> on the SEM analysis is stable, with a specific area of 240 m<sup>2</sup>/g and particle size of 15 nm. The stability of the nanoparticle size is very significant for the development of the nano-lubricant because the homogenisation process of nanoparticles and the base oil needs uniform nanoparticle sizes.



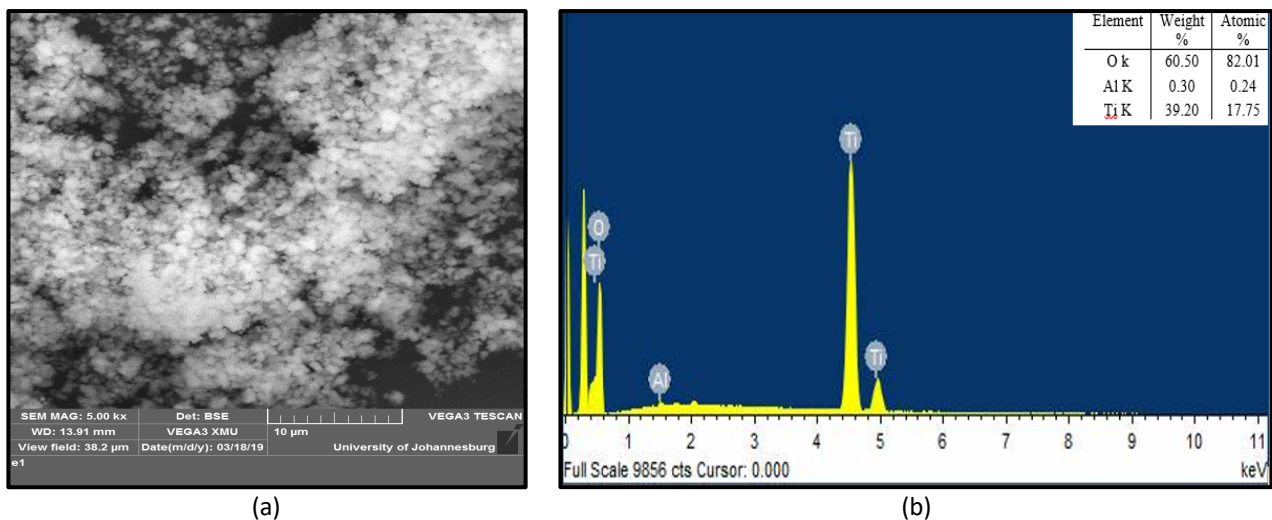


Fig. 2. (a) SEM micrograph of TiO<sub>2</sub> nano-powder, and (b) The EDS Analysis

The nonpolar saturated aliphatic and alicyclic hydrocarbons that make up white mineral oils are more refined versions of other mineral oils. They have no taste, odour, colour, or hydrophobicity, and their colour doesn't mutate over time.

## 2.2 Method

### 2.1.1 Procedures of synthesizing the nano-lubricant

When making nano-lubricants, two main methods—bottom-up, the one-step method of preparation, and top-down, sometimes known as the two-step approach—are always considered. The two-step method was used in this project. It is currently the most cost-effective method for mass-producing nano-lubricants. The nanoparticles were created in this process as dry powders using either physical or chemical means. Sigma-Aldrich Corporation manufactures the 99% pure TiO<sub>2</sub> used in this study. Using a micro-weighing scale, the % concentration of the nanoparticles was determined to be 0.2 g, 0.4 g, and 0.6 g for TiO<sub>2</sub>. The nanoparticles and mineral oil were homogenised for one hour and five hours using the magnetic stirrer and ultrasonic cleaning device. The generated nano-lubricants were then characterised using the SEM and EDS. Additionally, it is important to research physicochemical characteristics such as pH level, density, viscosity, stability, and refractive index before using nano-lubricants for machining operations.

### 2.1.2 Ultrasonic cleaner machine and the micro-scale device

The ultrasonic cleaning machine employed in this study is at the Department of Mechanical Engineering, Covenant University. The machine has a high occurrence of vibration when stirring the mixture. The water implementation in the ultrasonic bath assists in eliminating all traces of pollution or impurity from the embedded surface of the lubricant. Water is most frequently used, or the solvent is sometimes employed. The mixture in a beaker must not be placed in the ultrasonic bath alone without a solution. This will create a resistance that will not allow cavitation on the mixture or lubricant during the ultra-sonication process. The ultrasonic cleaner can be seen in Figure 3, along with other measuring instruments used for the mineral oil, such as the micro-milling scale for measuring the weight concentration of the TiO<sub>2</sub> and MWCNTs before the preparation of the nano-lubricant.

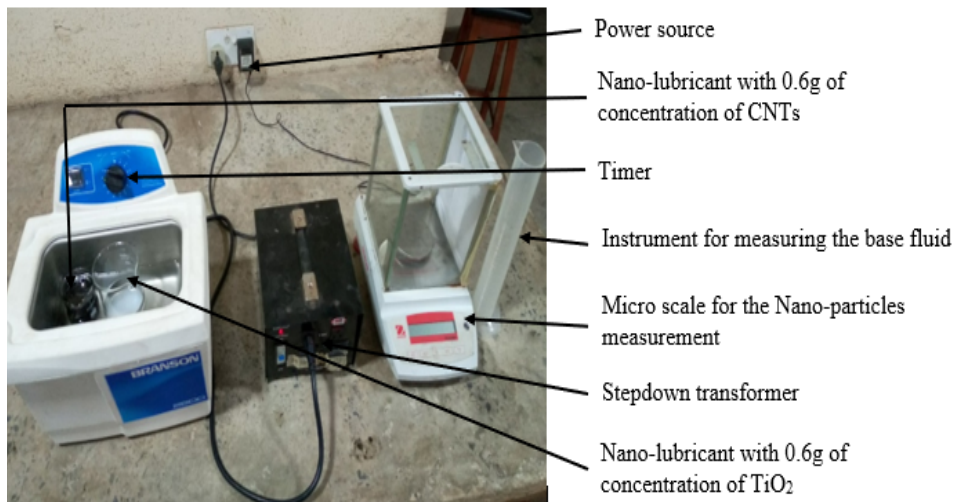


**Fig. 3.** Experimental setup for synthesising the TiO<sub>2</sub> nano-lubrication for the machining operation

### 2.1.3 Linear polarization resistance

The linear polarisation resistance (LPR) technique is employed to study the effect of the developed nano-lubricant on Al6061 alloy after machining. This technique is one of the most effective electrochemical processes for corrosion measurement. It gives the corrosion rate by determining the relationship between the current generated and the electrochemical potential. This non-destructive, quick-testing technique is commonly used in corrosion studies to capture data. The experimental setup of the LPR consists of three electrodes, a potentiostat, a regulator, and a computer system. The three electrodes are the working, reference, and counter electrodes. This analysis was conducted to ascertain whether the developed nano-lubricant is free from corrosion or resists corrosion during implementation. The experimental setup is presented in Figure 4.

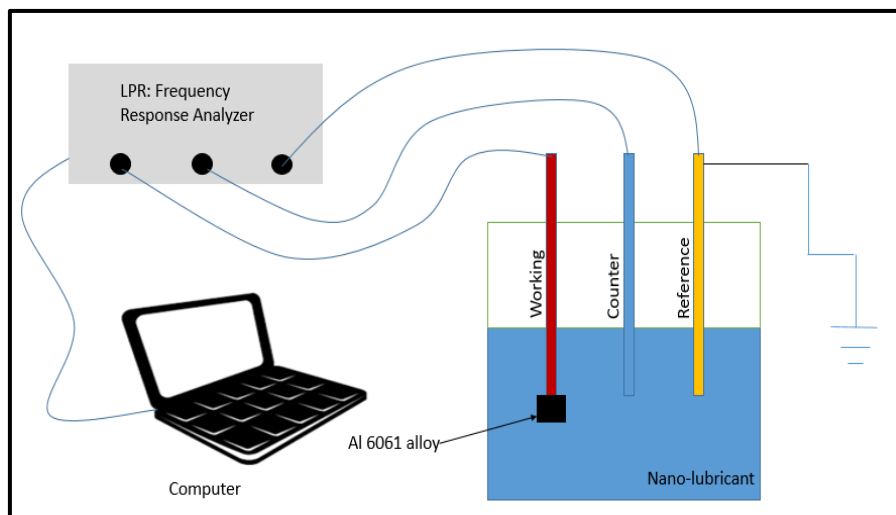


**Fig. 4.** Experimental setup of the surface corrosion test using the linear polarisation resistance method

The erosion studies to acquire consumption rate information were finished using weight reduction. This strategy was utilised because it is speedy and non-horrendous. The Al6061 alloy was separated into more modest coupons and marked for consumption testing, i.e., weight reduction in changed conditions. The weight reduction strategy is a quantitative method utilised in deciding and checking erosion, inner or outside, in metallic designs, in which case a metal half-breed composite. It includes taking readings of the distinctions in the heaviness of the metal under a concentration throughout unambiguous periods. It is considered the most straightforward erosion observation since it includes just time and weight factors, which are easy to acquire. The readings were required, like clockwork, for five days. The examples of the Al6061 alloy created were exposed to 5 conditions, as displayed in Table 2.

**Table 2**  
 Samples and their media

ENVIRONMENT	SPECIMEN
Soluble Oil	A1
Mineral Oil	A2
0.2g/L TiO <sub>2</sub> Nanomachining fluid	A3
0.4g/L TiO <sub>2</sub> Nanomachining fluid	A4
0.6g/L TiO <sub>2</sub> Nanomachining fluid	A5

Every example was eliminated from the climate it was exposed to the following 24 hours and was cleaned with a cloth so the contrast between their loads upon initiation and season of expulsion (following 24 hours) could be recorded and estimated. The weight estimation was finished utilising the OHAUS Advanced Gauging Scale. Why and how the conditions were ready: Soluble Oil Machining fluid: The coolant was prepared from 9g soluble oil and 500 ml distilled water. Mineral Oil: Mineral oil was purchased from the market. A coupon of the Al6061 alloy was submerged in 100ml of mineral oil to check for the reaction. The data obtained were entered into an engineering formula to generate Eq. (1) corrosion rates.

$$\text{Weight loss } (\Delta W = \text{Initial Weight } (W_i) - \text{Final weight after each time interval } (W_o)) \dots \quad (1)$$

The corrosion rate formula is shown in Eq. (2) and Eq. (3) [21]:

$$k = \frac{86.7 * \Delta W}{t * \rho * A} \quad (2)$$

Where;  $k$  = corrosion rate,  $\Delta W$  = weight loss,  $t$  = time,  $\rho$  = density,  $A$  = surface area

$$A = l * b * t \quad (3)$$

Where;  $l$  = length,  $b$  = breadth,  $t$  = thickness.

The Inhibition Efficiency formula is expressed below: Inhibition Efficiency= 100 x Surface Coverage  
 The Surface Coverage formula is given as:

$$SC = 1 - \frac{\Delta I}{\Delta_c} \quad (4)$$

Where;  $SC$  = Surface Coverage,  $\Delta_l$  = Weight loss of Al6061 alloy,  $\Delta_c$  = Weight loss of the Control sample

The experimental setup for the weight loss analysis is shown in Eq. (4):

#### 2.1.4 The Vickers hardness tester

The Vickers hardness tester employed in this work for the hardness measurement of the corrosive and non-corrosive Al6061 alloy sample is shown in Figure 10. The technique of the Vickers hardness test entails indenting the well-polished Al6061 alloy with a diamond indenter; the dwell time observed in this study is 15 seconds, with an angle of indentation of  $136^\circ$  between reverse faces subjected to a load of 1 to 100 kg. The surface of the well-polished Al6061 alloy is captured in ranges which are accurately controlled to the correct pyramid with a square base. The hardness test result is then determined from the diagonal between the two indentations left on the surface of the Al6061 alloy after eliminating the load.

#### 2.1.5 Microstructural analysis

The VEGA3 TESCAN scanning electron microscope (SEM) has an energy dispersive spectroscopy (EDS). The VEGA3 TESCAN is a multipurpose tungsten thermionic emission SEM for high and low vacuum processes. The SEM has various ports, five different chamber sizes, and optimised geometry for EDX with numerous detector methods. The process of obtaining the required image of the nanoparticles ( $TiO_2$ ), the nano-lubricant, the Al 6061 alloy, and the elemental chemical compositions were determined by applying EDS. All the samples are placed in the SEM sample holder and fixed to the SEM machine embedded with the EDS and the monitor (the software is installed to regulate the reflective analysis). The interaction between the cathode and anode in the elements present in the samples generates the workpiece's morphology and chemical composition. The techniques employed by XRD are constructive interference of monochromatic X-ray diffraction on the nanoparticles to determine the composition phase. This procedure revealed the crystalline structure of the experimental samples ( $TiO_2$  and MWCNTs nanoparticles). The X-ray detector then shows the result analysis by plotting the graph to show the peak intensity and  $2\theta$  ( $\theta$ ) angle. The X-ray diffraction (XRD) analysis of the phase transformation of the  $TiO_2$  nanoparticle is shown in Figure 5. The result indicates that at the  $2\theta$  degree of the sharp peaks of  $25.4^\circ$  and  $48^\circ$ , the 8000 and 2400 cps intensities showed that the  $TiO_2$  nanoparticles are anatase. The non-availability of indication of spurious diffractions in the XRD plot shows the level of crystallographic purity of the  $TiO_2$  nanoparticles. The XRD result also indicates that the  $TiO_2$  nanoparticles agree with the specification of the Joint Committee on Powder Diffraction Standards (JCPDS, card no 21-1272) [22].

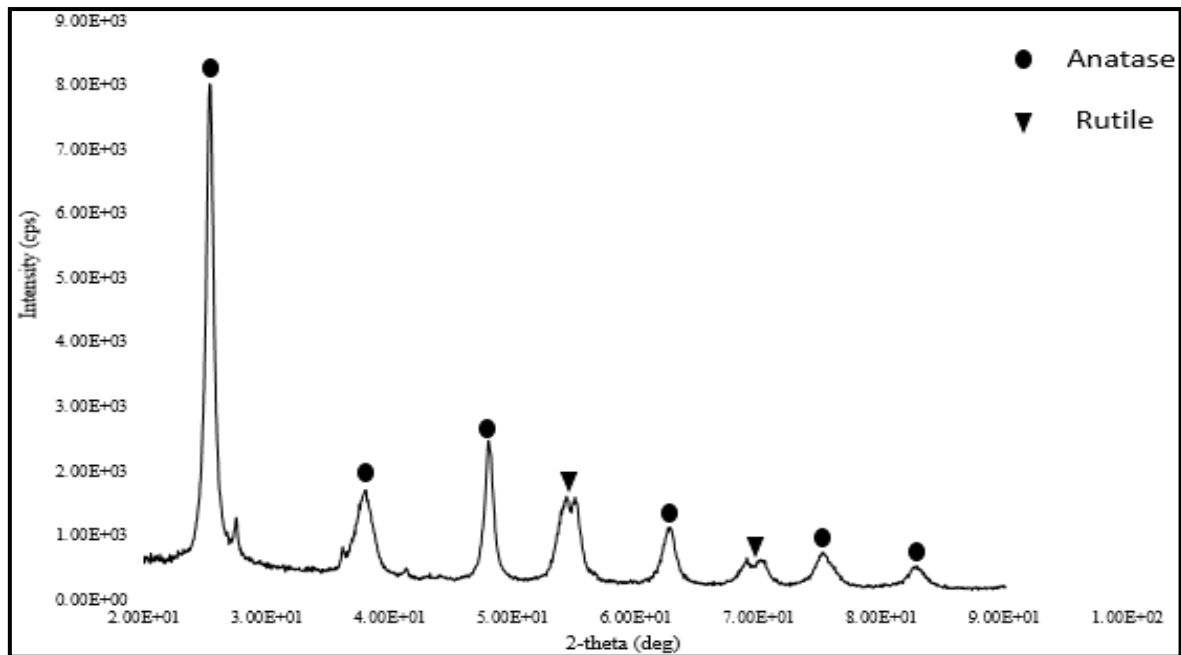


Fig. 5. XRD analysis of the TiO<sub>2</sub> nanoparticles employed in developing the nano-machining fluid

### 3. Results and Discussion

This section entails the results obtained from the experimental analysis of the corrosion study of the behaviour of Al 6061 alloys in various developed machining fluids. The section is divided into three (3) sections, which contain the surface hardness analysis, the microstructural analysis of the corrosion rate, and the polarisation resistances of the developed machining fluid towards the Al6061 alloys. After the corrosion study implementation, the advanced machining fluid was to ascertain its levels of eco-friendliness of the machining fluid before using it for manufacturing mechanical parts.

#### 3.1 The Effects of the Nano-Lubricant on the Surface Hardness after Machining Corrosion Analysis

A Vickers hardness tester was used to measure the workpiece's surface hardness after using the linear polarisation resistance (LPR) technique to submerge the Al 6061 alloys in the created machining fluid. Since the workpiece is an alloy of aluminium, the force is 500 N, and the dwell duration is 15 seconds. TiO<sub>2</sub> particles in mineral oil were developed into machining fluids with varying volume concentrations. To conduct a comparative analysis of the research on surface hardness, the five machining fluids were considered together with the samples that were initially provided (this is the current machining fluid used in most computer numerical control machines). In contrast, Sample A1 is the workpiece in its original condition, as received before corrosion studies were conducted. Sample A4 media contains 0.2 g/litre of TiO<sub>2</sub> nanoparticles, sample A5 media solution contains 0.4 g of TiO<sub>2</sub> nanoparticles, and sample A3 is the mineral oil environment. The fluid containing 0.6 g/litre of TiO<sub>2</sub> nanoparticles is sample A6. Figure 6 displays the hardness data from the various samples.

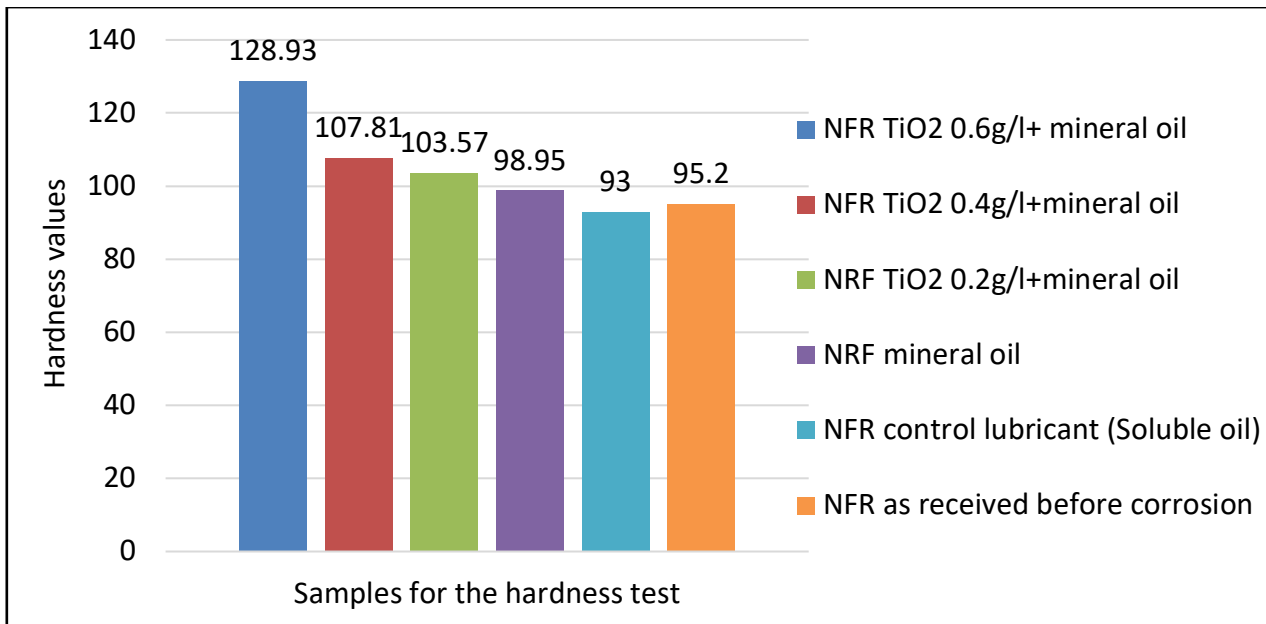


**Fig. 6.** The study of the surface hardness of the al 6061 alloys on the various machining fluid

Figure 6 demonstrates that after the workpiece was submerged in different fluid concentrations, the TiO<sub>2</sub> nanoparticles substantially impacted the surface hardness of the aluminium 6061 alloys. The trend of the results indicates that the surface hardness of alloy 6061 increases as the TiO<sub>2</sub> nanoparticle content rises. Additionally, it has been determined from the literature that the nanoparticles used in the machining process deposit a thin film of particles on the surface of the workpiece [23]. The nanoparticles help convert the sliding friction into a rolling process, thereby reducing the impact of the cutting tools on the workpiece, as shown in Figure 7. According to the analysis, the workpiece reacts with the soluble oil. It has a lower surface hardness compared to the control sample (A1), which has a surface hardness of 95.2, and sample A2 (soluble oil), which has a surface hardness of 93. According to the data, sample A6 has the highest surface hardness, measuring 128.93, followed by sample A5, weighing 0.4 g/litre, with a surface hardness of 107.81.

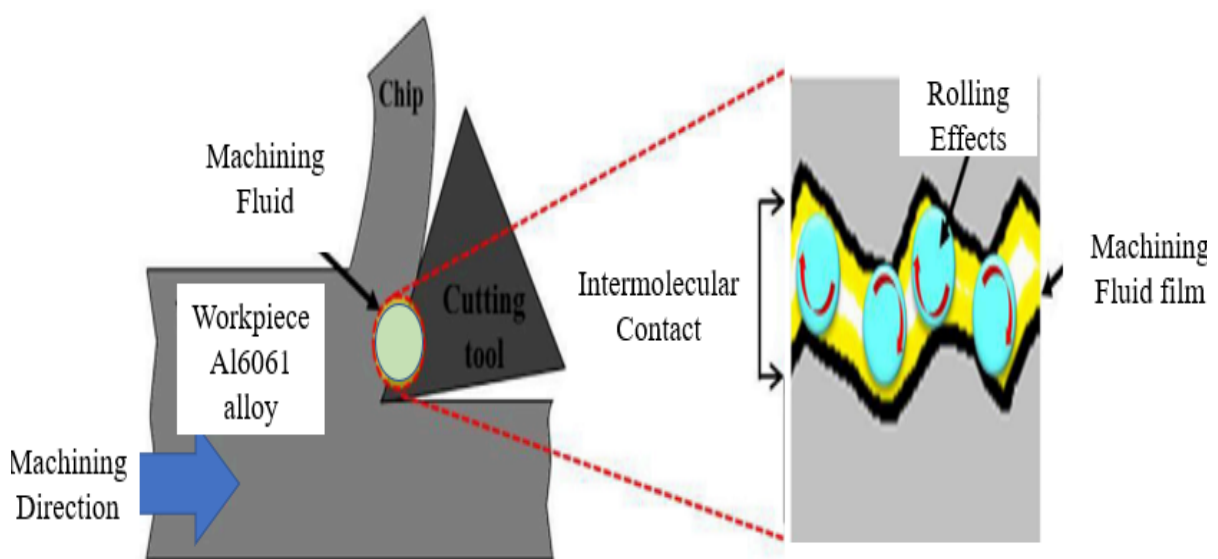


**Fig. 7.** Schematic illustration of interaction surfaces with the occurrence of TiO<sub>2</sub> nano-machining fluid

### 3.2 Microstructural Results from the Corrosion Analysis of the Al 6061 Alloy

The six-sample employed in this study, after the linear polarisation study, the samples were analysed to study the microstructural characteristic of the surface morphology using the VEGA3 TESCAN scanning electron microscope (SEM) equipped with the energy dispersive spectroscopy (EDS). Figure 8 is the as-received sample for the comparative analysis of the other five samples employed in the linear polarisation study.

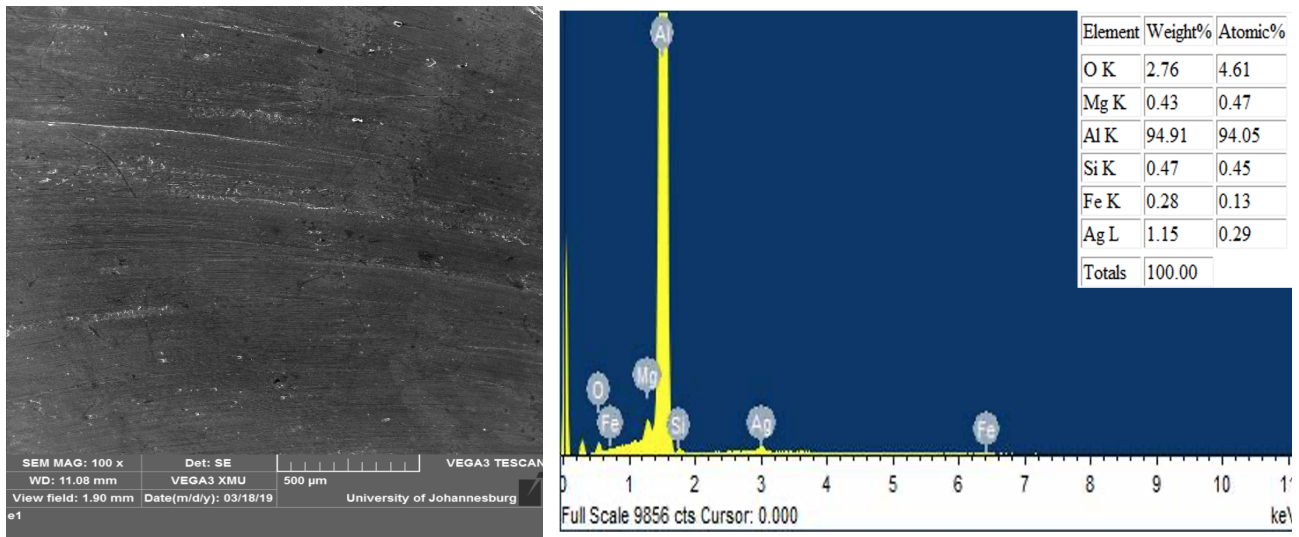


**Fig. 8.** SEM and EDS of the as-received AL 6061 alloy

Figure 9 presents sample A1 immersed in the soluble (control media) oil. The SEM image in Figure 9 shows that pit corrosion occurred in the normal face region, which can be seen with the dark spot.

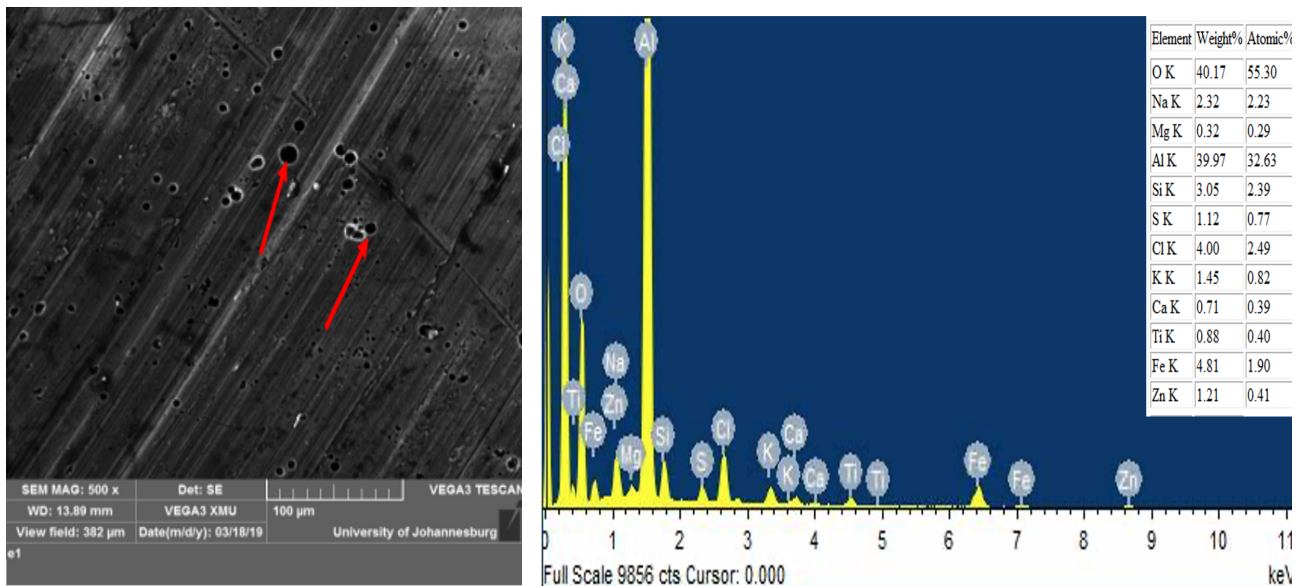


**Fig. 9.** The SEM and EDS analysis of the NFR (Sample A1) control lubricant (soluble oil) after LPR

Figure 9 debits the EDS analysis of sample A2 in the soluble oil media, which entails the elemental composition of the surface morphology of sample A2. It can be seen that 4% chlorine (Cl) and 2.32% sodium (Na) are presented, which can be the factor in why the pit corrosion occurs. The literature has also established that the machining fluid employed in the manufacturing industries is not



ecologically friendly to the operators and the workpiece. Moreover, when deposited in the environment, it causes environmental pollution.

Figure 10 shows both the SEM and EDS of the mineral oil media (sample A2) after the linear polarisation corrosion study. The normal face region offers a high rate of vibration, which can lead to tool wear substitution during the manufacturing process. Also, the EDS analysis proved that the mineral oil, when employed in the machining process, has a very low cooling rate, which causes high heat generation at the cutting region between the cutting tool and the workpiece by having an elemental composition of 3.3% oxygen, it can also be seen that the surface lubrication element is very low due to the present of 0.6% silicon.

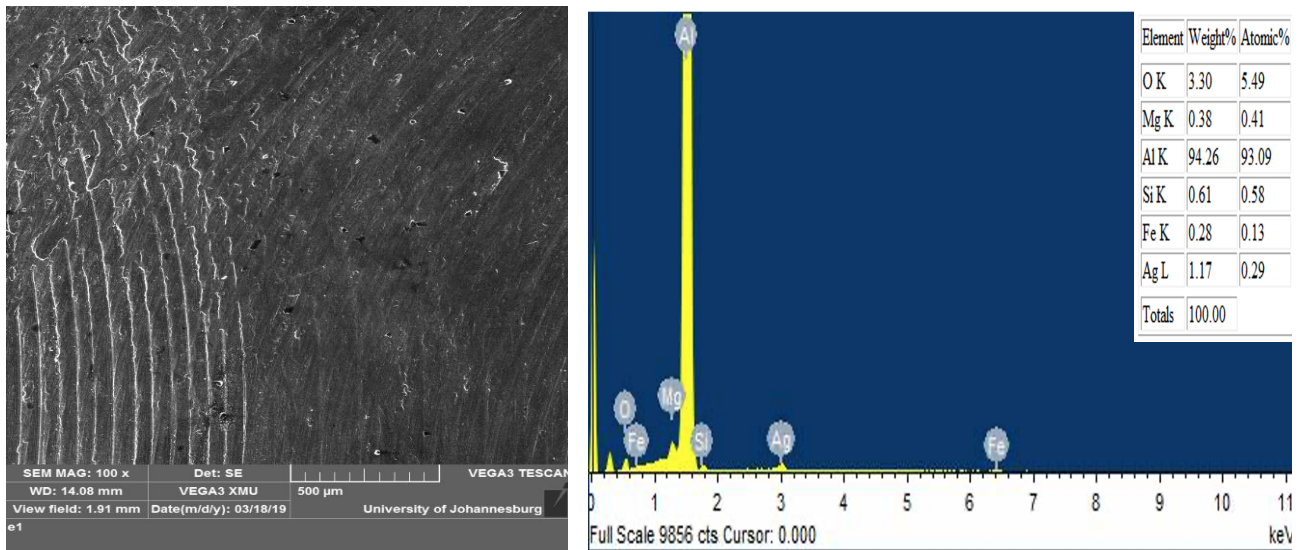


Fig. 10. The SEM and EDS analysis of the NFR (Sample A2) Mineral oil after LPR

Figure 11 shows the SEM and EDS analysis of the NFR (Sample A31) 0.2 g/litre TiO<sub>2</sub> lubricant after LPR. There is a trend in Figures 10, 11, and 12, which shows that the TiO<sub>2</sub> nanoparticles are present in the microstructural characteristics of samples A3-A5. The literature shows that during the machining process, the TiO<sub>2</sub> nanoparticles are deposited on the surface of the workpiece, thereby converting the sliding friction into rolling friction. Okokpujie *et al.* [24] show that applying the TiO<sub>2</sub> nanoparticles reduces the surface roughness, cutting force and temperature and improves the rheological property of the base oil employed in the study.

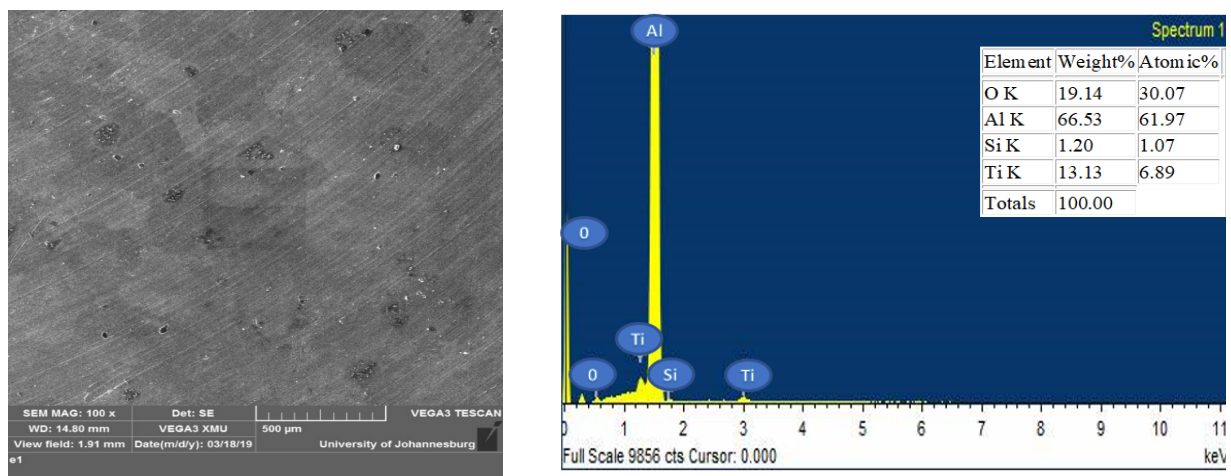


Fig. 11. The SEM and EDS analysis of the NFR (Sample A31) 0.2 g/litre TiO<sub>2</sub> lubricant after LPR



Figure 12 shows that the elemental compositions improve due to the implementation of the 0.2 g/l TiO<sub>2</sub> nanoparticles in the mineral oil compared with the pure mineral oil. Sample A3 has 19.14% Oxygen, 1.2% silicon, and 13.13% Titanium. However, as the TiO<sub>2</sub> nanoparticles increase to 0.4 g, the elemental composition of the cooling properties on the normal face region increases except silicon 30.24% Oxygen, 0.76% silicon, 18.23% Titanium and 50.78% aluminium. This analysis is present in Figure 12, giving the SEM and EDS analysis of the NFR (Sample A4) 0.4 g/litre nano-lubricant after LPR.

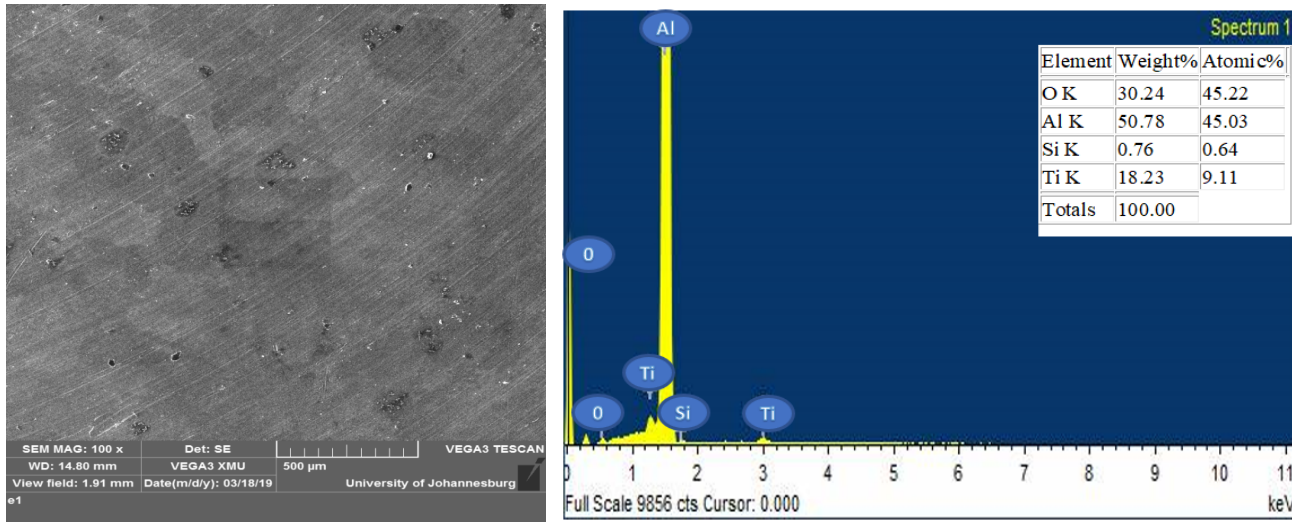


Fig. 12. The SEM and EDS analysis of the NFR (Sample A4) 0.4 g/litre nano-lubricant after LPR

Figure 13 shows the SEM and EDS analysis of the NFR (Sample A5) 0.6 g/litre nano-lubricant after LPR. The elemental composition obtained from the surface morphology analysis shows that the Oxygen in 0.4 g of TiO<sub>2</sub> media is higher than in the 0.6 g TiO<sub>2</sub> media. The elemental property of the 0.6 g TiO<sub>2</sub> is 25.29% Oxygen, 1.61% silicon, 1.48 calcium, 21.05% Titanium and 50.37% aluminium. This result is supported by observation, and the authors have drawn a colouration study to see that the reason for the increase in the surface hardness properties of sample A5 is a result of the presents of the TiO<sub>2</sub> nanoparticles deposited as a tiny film on the surface of the al 6061 alloys [26-28].

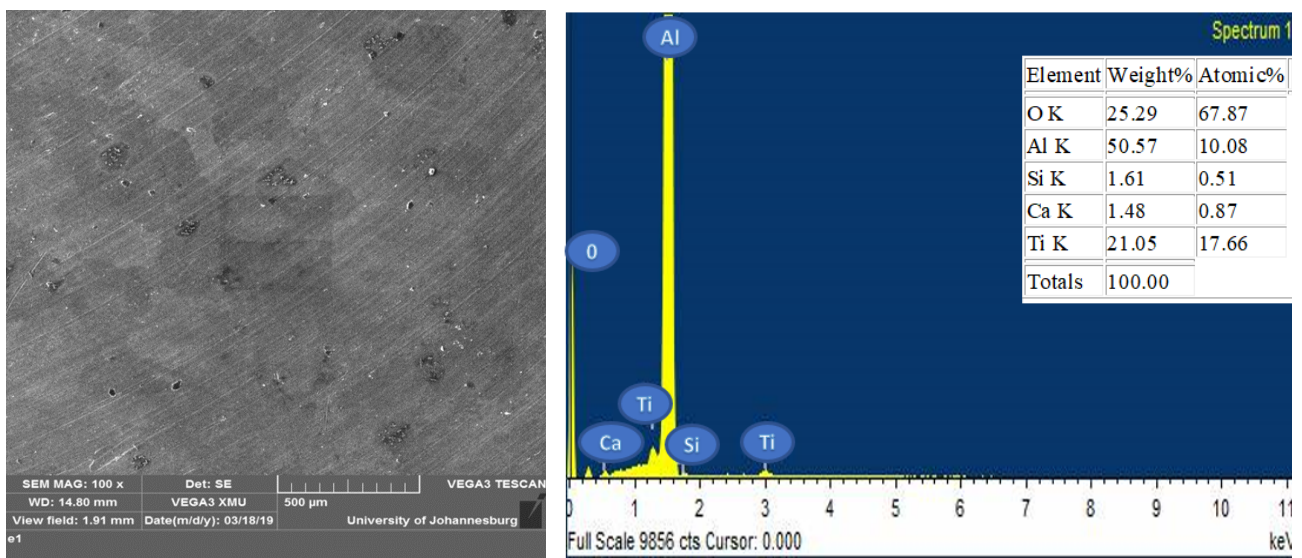


Fig. 13. The SEM and EDS analysis of the NFR (Sample A5) 0.6 g/litre nano-lubricant after LPR

### 3.3 Polarisation Analysis of the Corrosion Results of the Al 6061 Alloy in the Different Machining Fluid

The corrosion rate and the polarisation resistance results for the six samples are presented in Table 3. This analysis was conducted under the LSV staircase, with a start potential of  $-1.5 V_{ocp}$ , stop potential of  $1.5 V_{ocp}$ , scan rate of 0.01, and steps of 0.0025 V. The interval time is 0.244 seconds, the estimated number is 1229, and the estimated duration is 300.05. For the corrosion rate analysis, the Tafel analysis model, the environment's density is  $7.86 \text{ g/cm}^3$ , equivalent weight of  $27.925 \text{ g/mol}$  and surface area of  $1\text{cm}^2$ . From Table 3, it can be seen that there are significant differences in the corrosion rate and the polarisation resistance of the developed machining fluid.

**Table 3**

The Potentiodynamic corrosion and polarisation resistance for the various machining fluids under the normal face region (NFR) of the Al 6061 alloys

Samples	Ecorr. Obs. (V)	Jcorr. (A/cm <sup>2</sup> )	Icorr. (A)	Corrosion rate (μm/year)	Polarisation Resistance (MΩ)
NFR TiO <sub>2</sub> 0.6g/l+ mineral oil	-2.945	-9.856E-09	-9.857E-09	1.145	1.543
NFR TiO <sub>2</sub> 0.4g/l+mineral oil	-2.721	2.015E-09	2.015E-09	2.341	1.293
NRF TiO <sub>2</sub> 0.2g/l+mineral oil	-1.967	6.272E-08	6.272E-08	7.287	0.586
NRF mineral oil	-0.7252	5.722E-06	5.722E-06	55.489	0.455
NFR control lubricant	-0.721	8.984E-06	8.984E-06	104.393	0.406

Figure 14 and Figure 15 present the corrosion rate results and the linear polarisation resistance of the five (5) different media employed for this study. It can also be established that the increment of the TiO<sub>2</sub> nanoparticles in the corrosion analysis reduces the corrosion rate of the Al 6061 alloys [29,30]. The TiO<sub>2</sub> also act as an inhibitor for the polarisation resistance of the three (3) media that contain it. Corrosion rate (μm/year) 1.145, 2.341, 7.287, 55.489, and 104.393, respectively. Polarisation resistance (MΩ) 1.543, 1.293, 0.586, 0.455, and 0.406 for the five (5) samples, respectively.

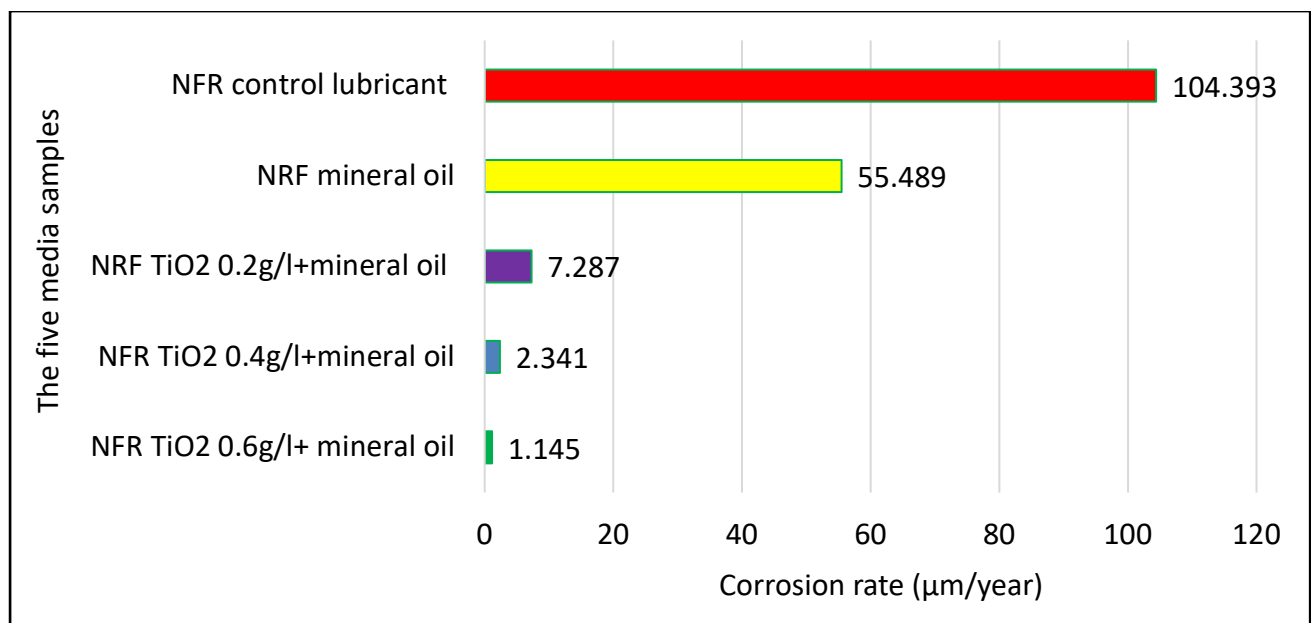


**Fig. 14.** The corrosion rate analysis for the developed machining fluid employed for the study

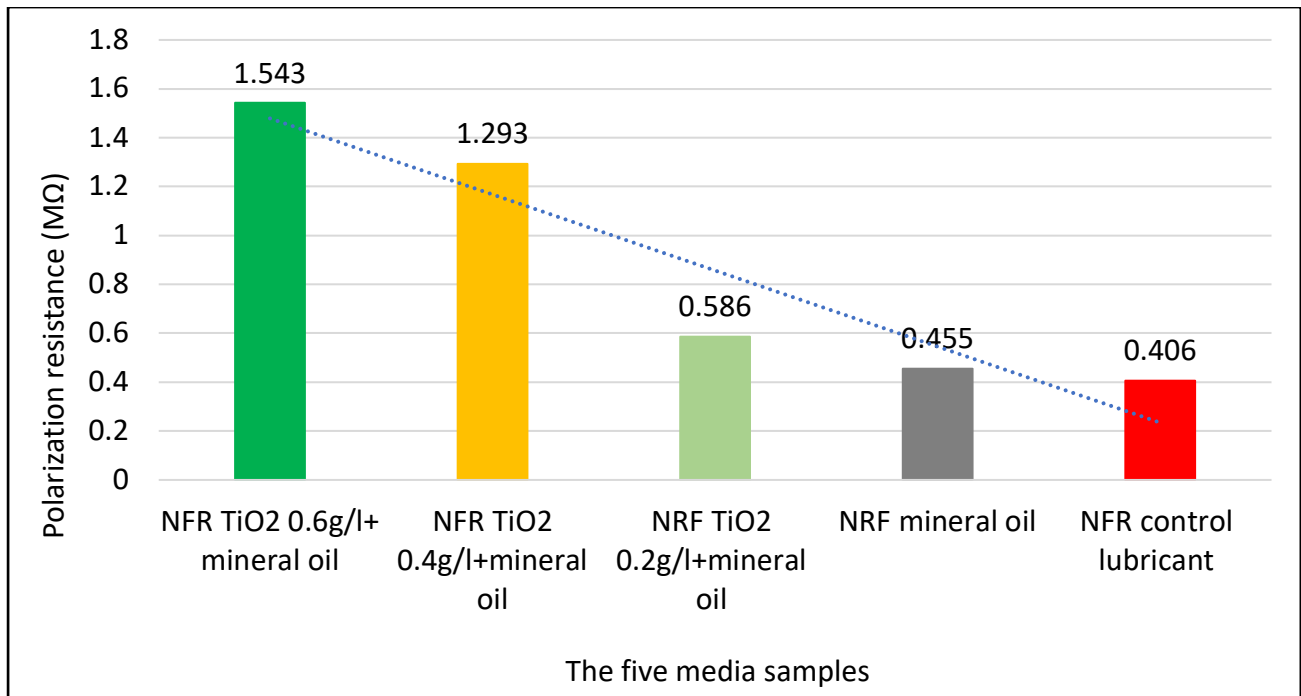


**Fig. 15.** The polarisation resistance analysis for the developed machining fluid employed for the corrosion study

#### 4. Conclusion

This project has successfully carried out an experimental study to analyse the effects of various machining fluids on the surface hardness and corrosion behaviour of al6061 alloy. This research developed five (5) different machining fluids via the two-step method of the nano-machining fluid process. The five samples are soluble oil (control sample) that is (sample A1), mineral oil (Sample A2) 0.2 g/litre TiO<sub>2</sub> nanoparticles (sample A3) 0.4 g/litre TiO<sub>2</sub> nanoparticles (sample A4), 0.6 g/litre TiO<sub>2</sub> nanoparticles (sample A5). After the preparation of the machining fluid, the project implements Potentiodynamic corrosion and polarization resistance to study the corrosion rate of the machining fluid on the surface of the al 6061 alloys, and after the corrosion study, the SEM and EDS to investigate the microstructure and elemental composition of the machining fluid and the Vickers micro-hardness for the hardness measurement, to enable the authors to carry out flexibility study of the behaviours of the various machining fluid on the surface hardness and corrosion rate on the al 6061 alloy. Therefore, the project has the following conclusions.

- i. The experimental study shows that adding the TiO<sub>2</sub> nanoparticles to the machining-based fluid increases the surface hardness. The pure sample A1, under the hardness analysis, has a hardness of 95.2, sample A2 93, sample A3 98.95, Sample A4 103.57, and Sample A 5107.81. sample A6 128.93 respectively.
- ii. The results of the corrosion rate and the linear polarisation resistances show that the media with 0.6 g of TiO<sub>2</sub> nanoparticles on the base machining fluid has the lowest corrosion rate of -1.145 (µm/year), the media of 0.4g TiO<sub>2</sub> nanoparticles has the corrosion rate of 2.341 (µm/year), media of 0.2 g TiO<sub>2</sub> nanoparticles has 7.287 (µm/year), corrosion rate. The mineral oil (55.489 µm/year) was also observed to reduce corrosion rate compared to soluble oil (104.393 µm/year).
- iii. This inhibitor act of the TiO<sub>2</sub> nanoparticles in the developed machining fluid also affected the linear polarisation resistance of the machining fluid. Polarisation resistance (MΩ)

1.543 (0.6 g TiO<sub>2</sub> nanoparticle), 1.293 (0.46 g TiO<sub>2</sub> nanoparticle), 0.586 (0.2 g TiO<sub>2</sub> nanoparticle), 0.455 (Mineral oil) and 0.406 (soluble oil) for the five (5) samples respectively.

## Acknowledgement

This research was not funded by any grant.

## References

- [1] Okokpuije, I. P., and L. K. Tartibu. "A mini-review of the behaviour characteristic of machining processes of aluminium alloys." *Materials Today: Proceedings* 62 (2022): 4526-4532. <https://doi.org/10.1016/j.matpr.2022.05.006>
- [2] Hutasoit, Novana, Muhammad Awais Javed, Rizwan Abdul Rahman Rashid, Scott Wade, and Suresh Palanisamy. "Effects of build orientation and heat treatment on microstructure, mechanical and corrosion properties of Al6061 aluminium parts built by cold spray additive manufacturing process." *International Journal of Mechanical Sciences* 204 (2021): 106526. <https://doi.org/10.1016/j.ijmecsci.2021.106526>
- [3] Sayuti, M., Ahmed AD Sarhan, and M. Hamdi. "An investigation of optimum SiO<sub>2</sub> nanolubrication parameters in end milling of aerospace Al6061-T6 alloy." *The International Journal of Advanced Manufacturing Technology* 67 (2013): 833-849. <https://doi.org/10.1007/s00170-012-4527-z>
- [4] Ajayi, Oluseyi O., Olasubomi F. Omowa, Oluwabunmi P. Abioye, Olugbenga A. Omotosho, Esther T. Akinlabi, Stephen A. Akinlabi, Abiodun A. Abioye, Felicia T. Owoeye, and Sunday A. Afolalu. "Finite element modelling of electrokinetic deposition of zinc on mild steel with ZnO-citrus sinensis as nano-additive." In *CFD Modeling and Simulation in Materials Processing 2018*, pp. 199-211. Springer International Publishing, 2018. [https://doi.org/10.1007/978-3-319-72059-3\\_19](https://doi.org/10.1007/978-3-319-72059-3_19)
- [5] Gavlas, Martin, Michal Kaco, Vladimír Dekýš, Miroslav Špiriak, Silvia Slabejová, Andrej Czán, Jozef Holubjak, Milena Kušnerová, Marta Harničárová, and Jan Valíček. "Research on the Oscillation in Centerless Grinding Technology When Machining Bearing Steel." *Materials* 15, no. 14 (2022): 4968. <https://doi.org/10.3390/ma15144968>
- [6] Venkatesh, K., G. Sriram, A. Uday Kiran Reddy, and S. V. R. Nikhil. "Influence of nano based metal working fluids on machining process—A Review." In *IOP Conference Series: Materials Science and Engineering*, vol. 390, no. 1, p. 012094. IOP Publishing, 2018. <https://doi.org/10.1088/1757-899X/390/1/012094>
- [7] Brinksmeier, E., D. Meyer, A. G. Huesmann-Cordes, and C. Herrmann. "Metalworking fluids—Mechanisms and performance." *CIRP Annals* 64, no. 2 (2015): 605-628. <https://doi.org/10.1016/j.cirp.2015.05.003>
- [8] Boye, Thank God E., Ojodomo J. Achadu, B. U. Oreko, and O. D. Samuel. "Carbon nanotubes: the building blocks of nanotechnology development." *Journal of Nanotechnology Progress International (JONPI)* 6, no. 2 (2016): 28-46.
- [9] Afolalu, Sunday A., Muoyowa Egbe, and Moses E. Emeter. "Development and Performance Evaluation of Silica Nano-Cutting Fluids From Rice Husk Ash (RHA) for Metalworking and Machining Operations." *Journal of Bio-and Tribo-Corrosion* 7 (2021): 1-9. <https://doi.org/10.1007/s40735-021-00582-9>
- [10] Okokpuije, Imhade P., Lagouge K. Tartibu, Jude E. Sinebe, Adeyinka OM Adeoye, and Esther T. Akinlabi. "Comparative study of rheological effects of vegetable Oil-Lubricant, TiO<sub>2</sub>, MWCNTs Nano-Lubricants, and machining parameters' influence on cutting force for sustainable metal cutting process." *Lubricants* 10, no. 4 (2022): 54. <https://doi.org/10.3390/lubricants10040054>
- [11] Akkurt, Adnan. "The effect of cutting process on surface microstructure and hardness of pure and Al 6061 aluminium alloy." *Engineering Science and Technology, an International Journal* 18, no. 3 (2015): 303-308. <https://doi.org/10.1016/j.jestch.2014.07.004>
- [12] Maurya, Saurabh Kumar, Prashant Chechi, Rabindra Prasad, Chander Kant Susheel, and Alakesh Manna. "Effect of surface finish on corrosion behavior of polished Al6061 alloy in simulated acid rain environment." *Materials Today: Proceedings* 64 (2022): 755-759. <https://doi.org/10.1016/j.matpr.2022.05.208>
- [13] C Ananda Murthy, H., and Somit Kumar Singh. "Influence of TiC particulate reinforcement on the corrosion behaviour of Al 6061 metal matrix composites." *Advanced Materials Letters* 6, no. 7 (2015): 633-640. <https://doi.org/10.5185/amlett.2015.5654>
- [14] Okokpuije, Imhade P., and Lagouge Tartibu. "Corrosion behaviour of coconut rice and eggshell reinforced aluminium metal matrix composites in 0.4 M H<sub>2</sub>SO<sub>4</sub>." *Advances in Materials and Processing Technologies* (2023): 1-15. <https://doi.org/10.1080/2374068X.2023.2192389>
- [15] Sen, Binayak, Mozammel Mia, Grzegorz M. Krolczyk, Uttam Kumar Mandal, and Sankar Prasad Mondal. "Eco-friendly cutting fluids in minimum quantity lubrication assisted machining: a review on the perception of



- sustainable manufacturing." *International Journal of Precision Engineering and Manufacturing-Green Technology* 8 (2021): 249-280. <https://doi.org/10.1007/s40684-019-00158-6>
- [16] Okokpujie, Imhade Princess, Omolayo M. Ikumapayi, Ugochukwu C. Okonkwo, Enesi Y. Salawu, Sunday A. Afolalu, Joseph O. Dirisu, Obinna N. Nwoke, and Oluseyi O. Ajayi. "Experimental and mathematical modeling for prediction of tool wear on the machining of aluminium 6061 alloy by high speed steel tools." *Open Engineering* 7, no. 1 (2017): 461-469. <https://doi.org/10.1515/eng-2017-0053>
- [17] Okokpujie, Imhade P., Jude E. Sinebe, Lagouge K. Tartibu, Adeyinka OM Adeoye, Sylvia E. Kelechi, and Esther T. Akinlabi. "Ratio Study of High-Pressure Lubrication and Cutting Parameters Effects on Machining Operations and Its Effect Towards Sustainable Machining: A Review." *Journal Européen des Systèmes Automatisés* 55, no. 2 (2022). <https://doi.org/10.18280/jesa.550206>
- [18] Padhan, Smita, Naresh Kumar Wagri, Lalatendu Dash, Anshuman Das, Sudhansu Ranjan Das, Mohammad Rafiqhi, and Priyaranjan Sharma. "Investigation on Surface Integrity in Hard Turning of AISI 4140 Steel with SPPP-ALTiSiN Coated Carbide Insert under Nano-MQL." *Lubricants* 11, no. 2 (2023): 49. <https://doi.org/10.3390/lubricants11020049>
- [19] Wagri, Naresh Kumar, Neelesh Kumar Jain, Anand Petare, Sudhansu Ranjan Das, Mohammed Y. Tharwan, Abdulkarim Alansari, Bader Alqahtani, Majed Fattouh, and Ammar Elsheikh. "Investigation on the Performance of Coated Carbide Tool during Dry Turning of AISI 4340 Alloy Steel." *Materials* 16, no. 2 (2023): 668. <https://doi.org/10.3390/ma16020668>
- [20] Wagri, Naresh Kumar, Anand Petare, Abhishek Agrawal, Ravi Rai, Rajkumar Malviya, Sunil Dohare, and Kamal Kishore. "An overview of the machinability of alloy steel." *Materials Today: Proceedings* 62 (2022): 3771-3781. <https://doi.org/10.1016/j.matpr.2022.04.457>
- [21] Okokpujie, Imhade P., Lagouge K. Tartibu, Kunle Babaremu, Collins Akinfaye, Adebayo T. Ogundipe, and Esther T. Akinlabi. "Study of the corrosion, electrical, and mechanical properties of aluminium metal composite reinforced with coconut rice and eggshell for wind turbine blade development." *Cleaner Engineering and Technology* 13 (2023): 100627. <https://doi.org/10.1016/j.clet.2023.100627>
- [22] Lu, P. J., S. W. Fang, W. L. Cheng, S. C. Huang, M. C. Huang, and H. F. Cheng. "Characterization of titanium dioxide and zinc oxide nanoparticles in sunscreen powder by comparing different measurement methods." *Journal of Food and Drug Analysis* 26, no. 3 (2018): 1192-1200. <https://doi.org/10.1016/j.jfda.2018.01.010>
- [23] Talib, N., and E. A. Rahim. "Experimental evaluation of physicochemical properties and tapping torque of hexagonal boron nitride in modified jatropha oils-based as sustainable metalworking fluids." *Journal of Cleaner Production* 171 (2018): 743-755. <https://doi.org/10.1016/j.jclepro.2017.10.061>
- [24] Okokpujie, I. P., C. A. Bolu, and O. S. Ohunakin. "Comparative performance evaluation of TiO<sub>2</sub> and MWCNTs nano-lubricant effects on surface roughness of AA8112 alloy during end-milling machining for sustainable manufacturing process." *The International Journal of Advanced Manufacturing Technology* 108 (2020): 1473-1497. <https://doi.org/10.1007/s00170-020-05397-5>
- [25] Shrivastava, Vikas, Pradeep Singh, Gaurav Kumar Gupta, Shashank Kumar Srivastava, and I. B. Singh. "Synergistic effect of heat treatment and reinforcement content on the microstructure and corrosion behavior of Al-7075 alloy based nanocomposites." *Journal of Alloys and Compounds* 857 (2021): 157590. <https://doi.org/10.1016/j.jallcom.2020.157590>
- [26] Hamrayev, Hemra, and Kamyar Shameli. "Synthesis and Characterization of Ionically Cross-Linked Chitosan Nanoparticles." *Journal of Research in Nanoscience and Nanotechnology* 7, no. 1 (2022): 7-13. <https://doi.org/10.37934/jrnn.7.1.713>
- [27] Kumar, Manoj, and Aadil Hashim Saifi. "Marangoni Convection in Liquid Bridges due to a Heater/Cooler Ring." *Journal of Advanced Research in Numerical Heat Transfer* 12, no. 1 (2023): 18-25.
- [28] El-Salamony, Mostafa E., Ernesto Benini, Osama A. Gaheen, and Mohamed A. Khalifa. "Cooling Strategies for Heated Cylinders Using Pulsating Airflow with Different Waveforms." *CFD Letters* 15, no. 9 (2023): 56-82. <https://doi.org/10.37934/cfdl.15.9.5682>
- [29] Mahbubah, N. A., M. Nuruddin, S. S. Dahda, D. Andesta, E. Ismiyah, D. Widyaningrum, M. Z. Fathoni *et al.*, "Optimization of CNC Turning Parameters for cutting Al6061 to Achieve Good Surface Roughness Based on Taguchi Method." *Journal of Advanced Research in Applied Mechanics* 99, no. 1 (2022): 1-9.
- [30] Arunkumar, T., Velmurugan Pavanan, Vijay Anand Murugesan, V. Mohanavel, and Karthikeyan Ramachandran. "Influence of nanoparticles reinforcements on aluminium 6061 alloys fabricated via novel ultrasonic aided rheo-squeeze casting method." *Metals and Materials International* 28, no. 1 (2022): 145-154. <https://doi.org/10.1007/s12540-021-01036-0>